Published for SISSA by Springer

Received: *July 29, 2025*
Revised: *October 6, 2025*
Accepted: *October 28, 2025*
Published: *December 3, 2025*

Search for the decay $B^0 \to \phi\phi$

The LHCb collaboration

E-mail: mary.richardson-slipper@cern.ch

Abstract: A search for the decay $B^0 \to \phi\phi$ is made using pp collision data collected with the LHCb detector at centre-of-mass energies of 7, 8 and 13 TeV, corresponding to an integrated luminosity of $9\,\text{fb}^{-1}$. No significant signal is observed, and an upper limit on the branching fraction of $1.3\ (1.4) \times 10^{-8}$ at 90 (95)% confidence level is set. This result supersedes the previous LHCb study and improves the upper limit by a factor of two.

Keywords: B Physics, Flavour Physics, Hadron-Hadron Scattering

ArXiv ePrint: 2507.20945

https://doi.org/10.1007/JHEP12(2025)026

JHEP12(2025)026

Contents

1 Introduction

In the Standard Model, the $B^0 \to \phi\phi$ decay proceeds via a loop-suppressed annihilation diagram that is subject to both Okubo-Zweig-Iizuka [1–3] and Cabibbo suppression [4]. Theoretical predictions for the branching fraction lie in the range $(0.5\text{–}5)\times10^{-8}$ [5–12]. The large spread in the predictions reflects the complexity of the perturbative QCD calculations as well as possible long-range contributions from $\omega - \phi$ mixing, rescattering and nonfactorizable diagrams that are difficult to estimate. The branching fraction may be enhanced by up to an order of magnitude in certain new physics models with additional Z bosons [7] or R-parity violating supersymmetry [8]. The first experimental searches for the $B^0 \to \phi\phi$ decay were carried out by the CLEO [13], SLD [14] and BaBar collaborations [15]. More recently, the LHCb collaboration set the most stringent limit to date, $\mathcal{B}(B^0 \to \phi\phi) < 2.7 \times 10^{-8}$ at 90% confidence level [16], using data collected between 2011 and 2016.

In this paper, a dedicated search is made for the $B^0 \to \phi\phi$ decay mode,[1] with the subsequent decay $\phi \to K^+K^-$, where ϕ implies the $\phi(1020)$ throughout. The abundant signal of the corresponding B^0_s mode provides an ideal control channel and normalisation mode, with branching fraction $\mathcal{B}(B^0_s \to \phi\phi) = (1.84 \pm 0.05\,(\text{stat}) \pm 0.07\,(\text{syst}) \pm 0.011\,(f_s/f_d) \pm 0.12\,(\text{norm})) \times 10^{-5}$ [17]. This study, which supersedes the previous LHCb result [16], uses the full dataset collected by the LHCb collaboration in proton-proton (pp) collisions between 2011 and 2018, which corresponds to an integrated luminosity of $3\,\text{fb}^{-1}$ collected at a centre-of-mass energies of $\sqrt{s} = 7$ and $8\,\text{TeV}$ (Run 1) and $6\,\text{fb}^{-1}$ collected at $\sqrt{s} = 13\,\text{TeV}$ (Run 2). The dataset used is a factor of two larger than that used in the previous LHCb study [16] which analysed only the data collected up to 2016. In addition, a more detailed understanding of background sources has allowed for significant reduction of the background, which further improves the sensitivity by a factor of 1.8. To avoid experimenter bias, the invariant-mass region around the B^0 mass was not examined until the full analysis procedure had been finalised.

[1] Charge conjugation is implied throughout.

JHEP12(2025)026

2 Detector and simulation

The LHCb detector [18, 19] is a single-arm forward spectrometer that covers the pseudorapidity range $2 < \eta < 5$, designed for the study of particles containing b or c quarks. The detector used for this analysis includes a high-precision tracking system consisting of a silicon-strip vertex detector surrounding the pp interaction region, a large-area silicon-strip detector located upstream of a dipole magnet with a bending power of approximately 4 T m, and three stations of silicon-strip detectors and straw drift tubes placed downstream of the magnet. The tracking system provides a measurement of the momentum, p, of charged particles with a relative uncertainty that varies from 0.5% at low momentum to 1.0% at $p = 200\,\text{GeV}/c$. Large samples of $B^+ \to J/\psi K^+$ and inclusive $J/\psi \to \mu^+\mu^-$ decays, collected concurrently with the dataset used in this analysis, are used to calibrate the momentum scale of the spectrometer [20]. The relative uncertainty achieved on the momentum scale is 3×10^{-4}.

Charged hadrons are distinguished using information from two ring-imaging Cherenkov (RICH) detectors. In addition, photons, electrons and hadrons are identified by a calorimeter system consisting of scintillating-pad and preshower detectors, an electromagnetic and a hadronic calorimeter. Muons are identified by a system composed of alternating layers of iron and multiwire proportional chambers.

The online event selection is performed by a trigger, which consists of a hardware stage followed by a two-level software stage [21, 22]. At the hardware trigger stage, events are required to have a muon with high transverse momentum or a hadron, photon or electron with high transverse energy in the calorimeters. For hadrons, the transverse energy threshold is 3.5 GeV. The software trigger requires a two-, three- or four-track secondary vertex with a significant displacement from any primary pp interaction vertex (PV). At least one charged particle must have a transverse momentum $p_{\mathrm{T}} > 1.6\,\text{GeV}/c$ and be inconsistent with originating from a PV. A multivariate algorithm [23, 24] is used for the identification of secondary vertices consistent with the decay of a b hadron. In the offline selection, trigger signals are associated with reconstructed particles. Selection requirements can therefore be made on the trigger selection itself and on whether the decision was due to the signal candidate (TOS) or other particles produced in the pp collision (TIS).

Simulation is used to determine selection requirements and to describe the invariant-mass distribution of the signal candidates. To accurately model the detector resolution, pp collisions are generated using Pythia [25, 26] with a specific LHCb configuration [27]. The decays of unstable particles are described by EvtGen [28], in which final-state radiation is generated using Photos [29]. The interaction of the generated particles with the detector, and its response, are implemented using the Geant4 toolkit [30, 31] as described in ref. [32]. The full detector simulation reproduces the mass resolution observed in the data for b-hadron decays at the level of 5% or better. Several sources of background are also studied using the RapidSim fast-simulation package [33].

JHEP12(2025)026

3 Classifier for controlling kaon interactions

Assuming a $B^0 \to \phi\phi$ branching fraction at the 10^{-8} level, the $B_s^0 \to \phi\phi$ decay proceeds with a rate approximately three orders of magnitude larger. This, combined with a mass resolution of $15\,\text{MeV}/c^2$ and $m(B_s^0) - m(B^0) = 87.22 \pm 0.12\,\text{MeV}/c^2$ [34] means it is important to control the tail of the B_s^0 mass distribution within the B^0 signal region. Simulation studies show that the tail is dominated by candidates where one or more kaons either decay in flight or interact hadronically within the tracking system. Suppression of decays-in-flight is possible by removing kaon candidates with associated activity in the muon detector. However, this requirement alone is not sufficient, as it does not reject either hadronic interactions or decays-in-flight outside the muon system acceptance.

A well-established technique to discriminate between muons and hadrons that decay in flight or interact is to identify breakpoints or discontinuities in the trajectory of the particle within the tracking system [35–37]. This approach is adopted here with the novelty that a multivariate technique is used to separate kaons with and without interactions. Using simulation, a gradient-boosted decision tree [38, 39] from the TMVA toolkit [40, 41] is used to train a classifier, I_{BDT}. The truth information available in the simulation allows for identification of kaons that have interacted within the tracking system volume. As input, the I_{BDT} classifier uses discriminating variables related to the track fit quality, the matching of the track segments upstream and downstream of the spectrometer magnet, the number of hits on the track and the track kinematics. These variables are chosen as they show good agreement between data and simulation for muons from the $B^+ \to J/\psi(\to \mu^+\mu^-)K^+$ decay chain which acts as a control channel. As shown in figure 1, good separation between kaons with and without interactions is achieved. The I_{BDT} score shows reasonable agreement between data and simulation for the muons from the $B^+ \to J/\psi K^+$ decay which are used as a proxy for non-interacted kaons. Requiring $I_{\text{BDT}} > -0.4$ rejects 89% of interacted kaons with an efficiency of 95% for non-interacted kaons.[2] The efficiency of the chosen requirement agrees between data and simulation at the level of 1%. The effect of the I_{BDT} requirement is shown for simulated $B_s^0 \to \phi\phi$ events in figure 2. It can be seen that after the I_{BDT} requirement the tails from $B_s^0 \to \phi\phi$ are significantly reduced. This is an appreciable improvement compared to the previous analysis [16] where these tails limited the sensitivity to a potential $B^0 \to \phi\phi$ signal.

4 Selection

The offline selection consists of a loose preselection, including the rejection of poorly reconstructed candidates that have interacted in the spectrometer. This is followed by requirements on two multivariate algorithms that efficiently reduce the combinatorial background while maintaining high signal efficiency.

The preselection requires four charged particles that have a good quality track fit [19], $p_{\text{T}} > 400\ \text{MeV}/c$ and that are well-identified as kaons by the RICH detectors. Kaons that interact within the tracking system are rejected by the I_{BDT} requirement, described in section 3, and also by requiring no associated activity in the muon stations. Fake tracks created by the reconstruction from random combinations of hits in the detector are suppressed

[2] Here, 'interacted' refers to kaons that have either interacted hadronically or decayed in flight.

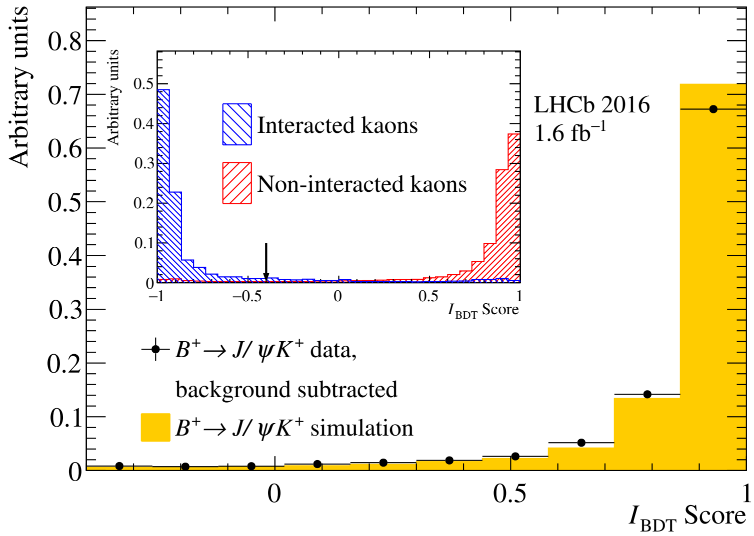

Figure 1. Distribution of the I_{BDT} classifier score for muons from the $B^+ \to J/\psi K^+$ decay in simulation and the LHCb 2016 data sample as an example. In the data, the combinatorial background has been subtracted using the technique described in ref. [42]. The statistical uncertainties on the data points are plotted but not visible. The inset figure shows the classifier response for interacted and non-interacted kaons in the $B_s^0 \to \phi\phi$ simulation samples used for training. The arrow on the inset figure indicates the imposed requirement.

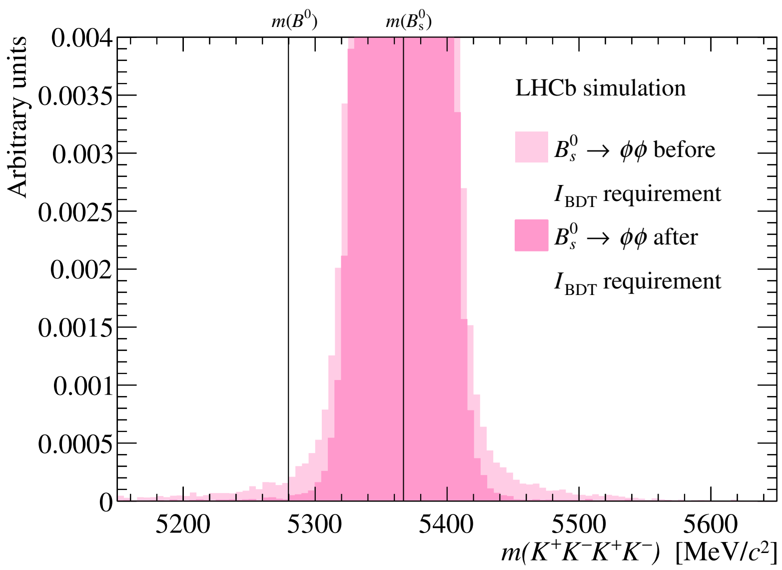

Figure 2. Four-kaon invariant-mass distribution of simulated $B_s^0 \to \phi\phi$ events shown before and after the application of the I_{BDT} requirement. The histograms are scaled such that the distribution before application of the classifier has unit area. The known B^0 and B_s^0 masses are indicated with solid black lines [34]. The full selection described in section 4 has been applied.

using a neural network trained to discriminate between these and genuine tracks associated to particles [43]. Oppositely charged kaon pairs that form a common vertex are combined to form ϕ candidates. Background from b-hadron decays with misidentified particles, such as $B^0 \to \phi K^{*0}$ and $\Lambda_b^0 \to \phi p K^-$, is strongly reduced by requiring the invariant mass of both K^+K^- pairs to be within $\pm 15\,\mathrm{MeV}/c^2$ of the known mass of the $\phi(1020)$ resonance [34].

Selected ϕ candidates are combined to form B candidates. To reduce combinatorial background, the product of the transverse momenta of the ϕ mesons is required to be greater than $1.2\,\mathrm{GeV}^2/c^2$ and that the reconstructed B decay time must exceed 0.3 ps. A vertex fit is performed on each candidate [44] requiring that the four tracks originate from a common point, and that the B candidate originates from the associated PV, chosen as the PV that best matches the flight direction of the B candidate. This fit is required to converge and a loose requirement is made on the χ^2 of this fit. To ensure good separation between B_s^0 and B^0 decays to the $\phi\phi$ final state, the estimated uncertainty on the mass of the B candidate is required to be less than $20\,\mathrm{MeV}/c^2$. Background from the $B^0 \to \phi K^*$ decay is suppressed by taking the kaon with the highest probability of being misidentified as a pion and assigning it the pion mass. If either $m(K^+\pi^-)$ is within $\pm 70\,\mathrm{MeV}/c^2$ of the known K^{*0} mass [34] or $m(K^+K^+K^+\pi^-)$ is within $\pm 30\,\mathrm{MeV}/c^2$ of the known B^0 mass, tighter particle-identification requirements are applied.

After applying these criteria, although the mass peak for B_s^0 signal is clearly visible, the combinatorial background due to random combinations of ϕ mesons is too large to give sufficient sensitivity for the B^0 search, and thus needs to be further reduced. Detached ϕ mesons are abundantly produced in D_s^+ meson decays. Since $\mathcal{B}(D_s^+ \to \phi X) = (15.7 \pm 1.0)\%$ [34], this decay is expected to be an important background source. Combining a candidate ϕ meson used to form a selected $B_{(s)}^0$ candidate with a high-p_T pion that is displaced from all PVs, a clear peak is seen at the D_s^+ mass, confirming this hypothesis. Candidate D_s^+ mesons selected in this way are used to train a gradient-boosted decision tree classifier [38, 39] from the TMVA toolkit [40, 41], referred to as the DBDT. This classifier is trained on data alone and is designed to select generic three-track combinations consistent with a D_s^+ decay. To determine the training weights a fit is made to the $K^+K^-\pi^+$ invariant-mass distribution and the sPlot technique [45] is used to separate signal and background. The classifier takes as input information related to the vertex fit χ^2, displacement from the PV and the pseudorapidity of the D_s^+ candidate. By making a requirement on DBDT and selecting the region around the known D_s^+ mass it is possible to cleanly identify and tag 90% of the background originating from a $D_s^+ \to \phi\pi^+$ decay, where the pion is reconstructed. The DBDT classifier also allows for the identification of $\phi\mu^+\nu_\mu$ and $\phi e^+\nu_e$ decays. In this case, since the neutrino is not reconstructed, only a loose requirement can be made on the ϕl^+ invariant mass. However, this is compensated by the lower combinatorial background for displaced high-p_T electrons or muons and this enables selection of these topologies with a low misidentification rate. In total, around 10% of the preselected candidates are identified as being from a D_s^+ decay. These candidates are referred to as D_s^+-tag background and are rejected with negligible loss in signal efficiency. The three decay modes considered account for around 50% of the inclusive branching fraction $\mathcal{B}(D_s^+ \to \phi X)$. The remainder of the branching fraction is dominated by modes with multiple charged or neutral pions, which cannot be cleanly identified. Given the D_s^+-tag only attempts to identify 50% of $D_s^+ \to \phi X$ decays and that the acceptance and reconstruction efficiency for the additional particle is $\sim 60\%$, a sizeable fraction of the remaining background is due to untagged candidates with this topology. Consequently, the D_s^+-tag sample is used, together with simulated $B_s^0 \to \phi\phi$ decays, to train a multilayer perceptron (MLP) from the TMVA toolkit [40]. This identifies $D_s^+ \to \phi X$ background candidates where no tag was possible. In the MLP, variables related to the B candidate isolation, the vertex fit χ^2 and the $\chi^2_{\rm IP}$ are used to discriminate between signal and background.[3] To allow for differences in data-taking conditions, separate classifiers are trained for the Run 1 and Run 2 datasets. The chosen requirement on the MLP output rejects 99.0% of the D_s^+-tag sample whilst keeping 97.5% of simulated signal candidates.

The final step of the selection procedure aims to discriminate between signal and generic combinatorial background. For this purpose, a gradient-boosted decision tree classifier (XBDT) is trained using the XGBoost package [46]. The training is performed separately for the TIS and TOS trigger categories, as they have different kinematic distributions and background levels, and also separately for the Run 1 and Run 2 data-taking periods. The classifier is trained using the $B_s^0 \to \phi\phi$ simulation samples as a proxy for the signal, and the B mass sidebands of the data as a proxy for the background. The sidebands are defined as $m(K^+K^-K^+K^-) < 5100$ MeV/c^2 or $m(K^+K^-K^+K^-) > 5650$ MeV/c^2. Only candidates passing a loose requirement on the MLP classifier score are used for training. This requirement was chosen to have sufficient background candidates for training while removing candidates that the MLP can easily classify as background. Variables related to the $B^0_{(s)}$ candidate kinematics, displacement, activity in the cone around the candidate [47], the isolation of the secondary vertex, the vertex fit χ^2, together with track fit χ^2 and particle-identification information of the kaons, are used in the training. All the variables used provide good separation between signal and background and agree well between data and simulation. As an example, figure 3 shows the classifier performance for the Run 2 TOS and TIS categories. To optimise the XBDT selection requirement for each category, the multicategory generalisation of the figure-of-merit described in refs. [48, 49] is used,

$$\mathrm{FOM} = \frac{A^2/B}{a/2 + A^{3/2}/B}, \tag{4.1}$$

with,

$$A = \sum_i \frac{\epsilon_i^2}{b_i} \quad , \quad B = \sum_i \frac{\epsilon_i^3}{b_i^2}, \tag{4.2}$$

where ϵ_i is the efficiency of the selection on signal in category i in $\{\mathrm{TIS}, \mathrm{TOS}\}$, b_i is the estimated background level in the invariant-mass region around the B^0 mass in category i with the parameter a set to 3, corresponding to a 3σ evidence. The chosen working points of the XBDT classifiers select signal with an overall efficiency of 92.7% and 82.6% in Run 1 and Run 2, respectively.

[3]The $\chi^2_{\rm IP}$ is defined as the difference in the vertex-fit χ^2 of a given PV reconstructed with and without the particle under consideration.

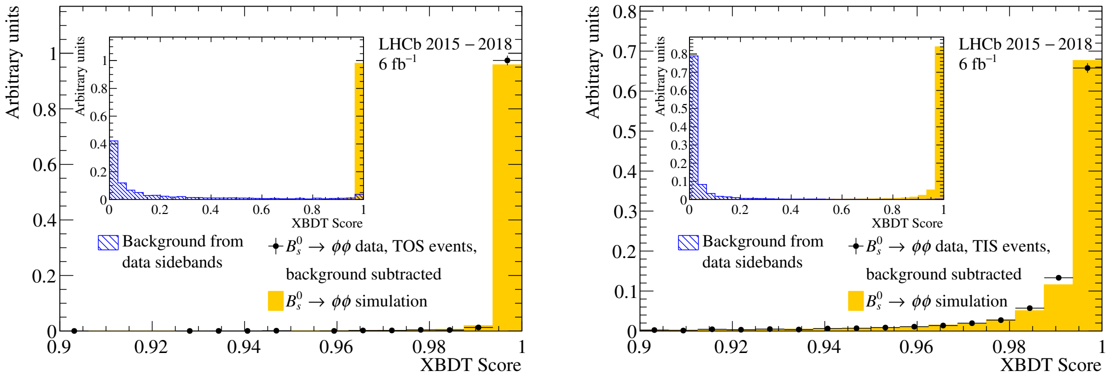

Figure 3. Response of the XBDT classifier for the Run 2 (left) TOS and (right) TIS categories for the $B_s^0 \to \phi\phi$ component in data (black points) and simulation (solid yellow). The response of the classifier on the background dataset used for training is shown in hatched blue in the inset plot. Combinatorial background in the data has been subtracted using the approach described in ref. [42].

5 Invariant-mass fit model

The simulation is used to develop invariant-mass models for the signal and background components for the Run 1 and Run 2 datasets. An important consideration in these studies is to ensure that the more abundant $B_s^0 \to \phi\phi$ decay is well described. Using the simulation, it is found that this component can be modelled by the sum of two Student's t-distributions [50] and a wide Gaussian component, with a common mean. The Gaussian component accounts for the remaining tail from interacted kaons. When fitting the data, the common mean and the n-parameter of the narrower Student's t-distribution are left free for the B_s^0 component. The n-parameter of the wider Student's t-distribution together with the width from the Gaussian function are constrained with Gaussian priors based on simulation fits, while the remaining parameters are fixed to the simulation values. The same model is used for the possible $B^0 \to \phi\phi$ component. In that case, the mean is constrained using the known $B^0 - B_s^0$ mass splitting [34], while the resolution of each of the Student's t-distributions is constrained via a Gaussian prior centered on the resolution of the B_s^0 component, with a scale factor of 0.996 ± 0.003 determined from the simulation.

Several background contributions are included in the invariant-mass model. The dominant background source is combinatorial and is modelled using an exponential function. As an alternative, a power law model is considered and found to give consistent results. Background from $\Lambda_b^0 \to \phi p K^-$ and $\Xi_b^0 \to \phi p K^-$ decays, where the proton is misidentified as a kaon, gives a broad shoulder to the right of the B_s^0 mass peak. Using the simulation, the shape of these components is found to be well described by Crystal Ball functions [51]. The yield of these components is estimated using data enriched in misidentified particles, obtained by selecting events that do not satisfy the particle-identification criteria used to separate kaons from protons. The number of rejected background candidates is estimated from data that fail the particle-identification criteria used to select the signal and then multiplied by the pass-fail factor obtained from a simulated sample of $\Lambda_b^0 \to \phi p K^-$ decays. This is done separately for Run 1 and Run 2 and the results applied as a Gaussian constraint on the yield

JHEP12(2025)026

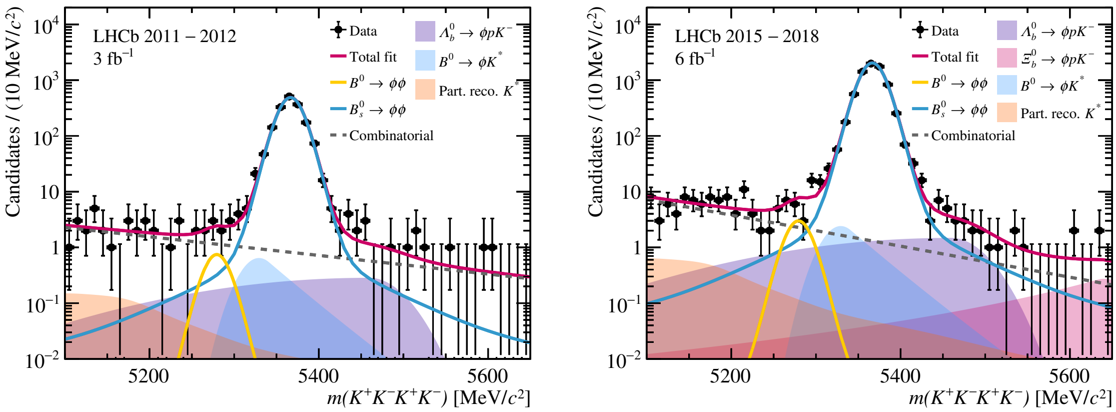

Figure 4. Four-kaon invariant-mass distribution for the (left) Run 1 and (right) Run 2 datasets. The fit result is also shown.

of this component in data. The remaining background from $B^0 \to \phi K^*(892)^0$ decays, with a misidentified pion, is modelled with a Crystal Ball function using simulation. The yield of this component is constrained relative to the $B_s^0 \to \phi\phi$ signal using the relative efficiency from the simulation and the known branching fractions. The yields relative to the $B_s^0 \to \phi\phi$ signal are constrained to $(24 \pm 4) \times 10^{-4}$ and $(22 \pm 2) \times 10^{-4}$ in Run 1 and Run 2, respectively. Finally, partially reconstructed background from b-hadron decays to charged and neutral $K_1(1270)$ and $K_2^*(1430)$ intermediate states is studied and modelled with a kernel estimation probability density function [52] using samples generated with RapidSim [33]. In the data fit the yield of this component is constrained using the known branching fractions and relative efficiency from the simulation. The yield relative to the $B_s^0 \to \phi\phi$ signal is constrained to $(12 \pm 2) \times 10^{-4}$.

The adopted fit model has been extensively validated using pseudoexperiments. In particular, it has been verified that the model is unbiased and does not generate a spurious signal following the procedure outlined in ref. [53].

6 Results and conclusions

To determine the $B^0 \to \phi\phi$ signal yield, an extended unbinned maximum-likelihood fit with the model described in section 5 is performed to the Run 1 and Run 2 datasets simultaneously. The yield of $B_s^0 \to \phi\phi$ events is free to vary in the fit. The yields for the background components are calculated separately for Run 1 and Run 2 while all shapes are shared except the combinatorial background. The results of this fit are shown in figure 4. The fit yields 2.6 ± 1.5 and 10.5 ± 6.3 signal decays for the Run 1 and Run 2 datasets, respectively, where the uncertainties quoted are statistical only. The results are consistent with the background-only hypothesis at the 1.9σ level. Hence, limits are set using the CL$_s$ method [54] with a one-sided test statistic, evaluated using pseudoexperiments. Systematic effects from modelling the signal and background components and knowledge of external branching fractions are included in the limit via Gaussian constraints. The largest source of systematic uncertainty comes from the $B_s^0 \to \phi\phi$ branching fraction which has a relative uncertainty of 7.7%. The uncertainty

JHEP12(2025)026

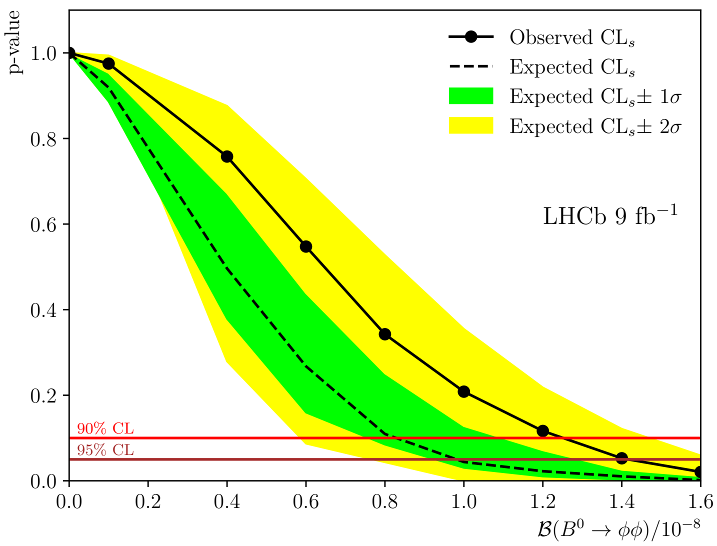

Figure 5. Results of the CL$_s$ method for setting an upper limit on the $B^0 \to \phi\phi$ branching fraction.

on the selection efficiency ratio gives a relative uncertainty of 0.5% on the central value due to the limited size of simulation samples. Since the limit on the $B^0 \to \phi\phi$ branching fraction is calculated with respect to the $B_s^0 \to \phi\phi$ decay with the same final state, several sources of systematic uncertainty cancel in the ratio. This includes systematic uncertainties due to tracking, particle identification and trigger efficiencies. The measured $B^0 \to \phi\phi$ yield, N_{B^0}, is converted into a branching fraction using

$$\mathcal{B}(B^0 \to \phi\phi) = \frac{N_{B^0}}{N_{B_s^0}} \cdot \frac{\epsilon_{B_s^0 \to \phi\phi}}{\epsilon_{B^0 \to \phi\phi}} \cdot \mathcal{B}(B_s^0 \to \phi\phi) \cdot f_s/f_d,$$

where $N_{B_s^0}$ is the $B_s^0 \to \phi\phi$ yield, f_s/f_d is the ratio of the fragmentation fractions and $\mathcal{B}(B_s^0 \to \phi\phi) = (1.84 \pm 0.05\ (\text{stat}) \pm 0.07\ (\text{syst}) \pm 0.011\,(f_s/f_d)\ \pm 0.12\,(\text{norm})) \times 10^{-5}$ [17]. The calculation takes into account the correlation between the external LHCb measurements, including those reported in [17]. In particular, the contribution of $f_s/f_d = 0.259 \pm 0.015$ cancels in the calculation given the decay $B^0 \to \phi K^{*0}$ was used for normalisation in ref. [17] where the $B_s^0 \to \phi\phi$ branching fraction is measured, giving $\mathcal{B}(B_s^0 \to \phi\phi) \cdot (f_s/f_d) = (477 \pm 37) \times 10^{-8}$. The ratio of efficiencies, $\epsilon_{B^0 \to \phi\phi}/\epsilon_{B_s^0 \to \phi\phi}$, is evaluated using the simulation to be 1.006 ± 0.006 for Run 1 and 0.971 ± 0.003 for Run 2, where the uncertainties are statistical only.

The result of the CL$_s$ calculation is shown in figure 5. The limits obtained are

$$\mathcal{B}(B^0 \to \phi\phi) < 1.3\ (1.4) \times 10^{-8} \text{ at } 90\%\ (95\%) \text{ confidence level.}$$

The obtained limit is found to be robust to changes in the signal and background modelling in the fit. For example, changing the combinatorial background model, the constraints applied to the signal line shape parameters, the modelling of the $\Lambda_b^0 \to \phi p K^-$ component and the partially reconstructed component all have no impact on the result. Additionally, relaxing the constraint on the width of the shallow Gaussian component of the signal model has a

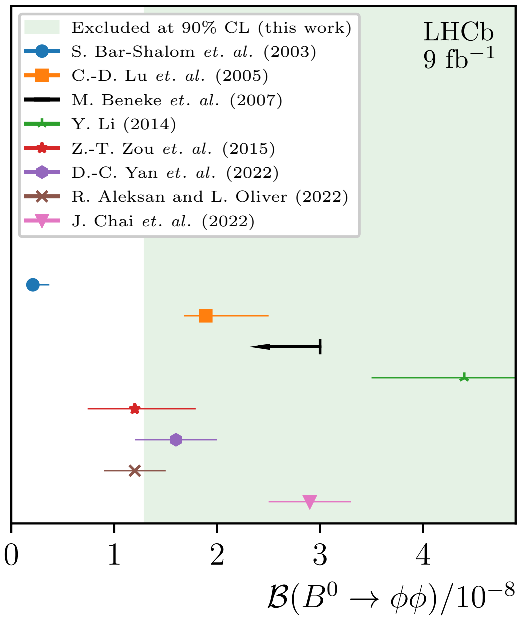

Figure 6. Limit set on $\mathcal{B}(B^0 \to \phi\phi)$ in this analysis at 90% confidence level compared to theoretical predictions. The results presented in this paper are represented by the shaded region.

negligible impact on the result. The result favours the lower end of the range of current predictions for the branching fraction (figure 6) and strongly constrains possible enhancements due to physics beyond the Standard Model. It supersedes the previous LHCb limit, presented in ref. [16], improving on it by a factor of two. Further improvements to this limit or evidence for this decay mode will be possible using the larger data set that is being collected by the upgraded LHCb experiment. Those studies will benefit from the improved understanding of the experimental backgrounds achieved in this analysis.

Acknowledgments

We express our gratitude to our colleagues in the CERN accelerator departments for the excellent performance of the LHC. We thank the technical and administrative staff at the LHCb institutes. We acknowledge support from CERN and from the national agencies: ARC (Australia); CAPES, CNPq, FAPERJ and FINEP (Brazil); MOST and NSFC (China); CNRS/IN2P3 (France); BMFTR, DFG and MPG (Germany); INFN (Italy); NWO (Netherlands); MNiSW and NCN (Poland); MCID/IFA (Romania); MICIU and AEI (Spain); SNSF and SER (Switzerland); NASU (Ukraine); STFC (United Kingdom); DOE NP and NSF (U.S.A.). We acknowledge the computing resources that are provided by ARDC (Australia), CBPF (Brazil), CERN, IHEP and LZU (China), IN2P3 (France), KIT and DESY (Germany), INFN (Italy), SURF (Netherlands), Polish WLCG (Poland), IFIN-HH (Romania), PIC (Spain), CSCS (Switzerland), and GridPP (United Kingdom). We are indebted to the communities behind the multiple open-source software packages on which we depend. Individual groups or members have received support from Key Research Program of Frontier Sciences of

JHEP12(2025)026

CAS, CAS PIFI, CAS CCEPP, Fundamental Research Funds for the Central Universities, and Sci. & Tech. Program of Guangzhou (China); Minciencias (Colombia); EPLANET, Marie Skłodowska-Curie Actions, ERC and NextGenerationEU (European Union); A*MIDEX, ANR, IPhU and Labex P2IO, and Région Auvergne-Rhône-Alpes (France); Alexander-von-Humboldt Foundation (Germany); ICSC (Italy); Severo Ochoa and María de Maeztu Units of Excellence, GVA, XuntaGal, GENCAT, InTalent-Inditex and Prog. Atracción Talento CM (Spain); SRC (Sweden); the Leverhulme Trust, the Royal Society, UKRI and IOP BBGSF (United Kingdom).

Data Availability Statement. Data associated to the plots in this publication as well as in supplementary materials are made available on the CERN document server at https://cds.cern.ch/record/2939205.

Code Availability Statement. This article has no associated code or the code will not be deposited.

References

[1] S. Okubo, *ϕ-meson and unitary symmetry model*, Phys. Lett. **5** (1963) 165 [INSPIRE].

[2] G. Zweig, *An SU(3) model for strong interaction symmetry and its breaking. Version 2*, in *Developments in the quark theory of hadrons. Volume 1. 1964–1978*, D.B. Lichtenberg and S.P. Rosen eds., (1964), p. 22–101 [DOI:10.17181/CERN-TH-412] [INSPIRE].

[3] J. Iizuka, *Systematics and phenomenology of meson family*, Prog. Theor. Phys. Suppl. **37** (1966) 21 [INSPIRE].

[4] N. Cabibbo, *Unitary symmetry and leptonic decays*, Phys. Rev. Lett. **10** (1963) 531 [INSPIRE].

[5] M. Beneke, J. Rohrer and D. Yang, *Branching fractions, polarisation and asymmetries of $B \to VV$ decays*, Nucl. Phys. B **774** (2007) 64 [hep-ph/0612290] [INSPIRE].

[6] C.-D. Lu, Y.-L. Shen and J. Zhu, *$B^0 \to \phi\phi$ decay in perturbative QCD approach*, Eur. Phys. J. C **41** (2005) 311 [hep-ph/0501269] [INSPIRE].

[7] Y. Li, *Investigating the effect of family non-universal Z' boson in $B \to \phi\phi$ decay*, Phys. Rev. D **89** (2014) 014003 [arXiv:1311.2664] [INSPIRE].

[8] S. Bar-Shalom, G. Eilam and Y.-D. Yang, *$B \to \phi\pi$ and $B^0 \to \phi\phi$ in the standard model and new bounds on R parity violation*, Phys. Rev. D **67** (2003) 014007 [hep-ph/0201244] [INSPIRE].

[9] Z.-T. Zou et al., *Improved estimates of the $B_{(s)} \to VV$ decays in perturbative QCD approach*, Phys. Rev. D **91** (2015) 054033 [arXiv:1501.00784] [INSPIRE].

[10] J. Chai et al., *Charmless two-body B meson decays in the perturbative QCD factorization approach*, Chin. Phys. C **46** (2022) 123103 [arXiv:2207.04190] [INSPIRE].

[11] D.-C. Yan, Z. Rui, Z.-J. Xiao and Y. Li, *Study of $B_s^0 \to \phi\phi \to (K^+K^-)(K^+K^-)$ decays in the perturbative QCD approach*, Phys. Rev. D **105** (2022) 093001 [arXiv:2204.01092] [INSPIRE].

[12] R. Aleksan and L. Oliver, *Remarks on the penguin decay $B_s \to \phi\phi$ with prospects for FCCee*, arXiv:2205.07823 [INSPIRE].

JHEP12(2025)026

[13] CLEO collaboration, *Observation of $B^+ \to \omega K^+$ and search for related B decay modes*, *Phys. Rev. Lett.* **81** (1998) 272 [hep-ex/9803018] [INSPIRE].

[14] SLD collaboration, *Search for charmless hadronic decays of B mesons with the SLD detector*, *Phys. Rev. D* **62** (2000) 071101 [hep-ex/9910050] [INSPIRE].

[15] BaBar collaboration, *Searches for B meson decays to $\phi\phi$, $\phi\rho$, $\phi f_0(980)$, and $f_0(980) f_0(980)$ final states*, *Phys. Rev. Lett.* **101** (2008) 201801 [arXiv:0807.3935] [INSPIRE].

[16] LHCb collaboration, *Measurement of CP violation in the $B_s^0 \to \phi\phi$ decay and search for the $B^0 \to \phi\phi$ decay*, *JHEP* **12** (2019) 155 [arXiv:1907.10003] [INSPIRE].

[17] LHCb collaboration, *Measurement of the $B_s^0 \to \phi\phi$ branching fraction and search for the decay $B^0 \to \phi\phi$*, *JHEP* **10** (2015) 053 [arXiv:1508.00788] [INSPIRE].

[18] LHCb collaboration, *The LHCb detector at the LHC*, 2008 *JINST* **3** S08005 [INSPIRE].

[19] LHCb collaboration, *LHCb detector performance*, *Int. J. Mod. Phys. A* **30** (2015) 1530022 [arXiv:1412.6352] [INSPIRE].

[20] LHCb collaboration, *Momentum scale calibration of the LHCb spectrometer*, 2024 *JINST* **19** P02008 [arXiv:2312.01772] [INSPIRE].

[21] R. Aaij et al., *The LHCb trigger and its performance in 2011*, 2013 *JINST* **8** P04022 [arXiv:1211.3055] [INSPIRE].

[22] LHCb collaboration, *Design and performance of the LHCb trigger and full real-time reconstruction in run 2 of the LHC*, 2019 *JINST* **14** P04013 [arXiv:1812.10790] [INSPIRE].

[23] V.V. Gligorov and M. Williams, *Efficient, reliable and fast high-level triggering using a bonsai boosted decision tree*, 2013 *JINST* **8** P02013 [arXiv:1210.6861] [INSPIRE].

[24] T. Likhomanenko et al., *LHCb topological trigger reoptimization*, *J. Phys. Conf. Ser.* **664** (2015) 082025 [arXiv:1510.00572] [INSPIRE].

[25] T. Sjöstrand, S. Mrenna and P.Z. Skands, *A brief introduction to PYTHIA 8.1*, *Comput. Phys. Commun.* **178** (2008) 852 [arXiv:0710.3820] [INSPIRE].

[26] T. Sjöstrand, S. Mrenna and P.Z. Skands, *PYTHIA 6.4 physics and manual*, *JHEP* **05** (2006) 026 [hep-ph/0603175] [INSPIRE].

[27] LHCb collaboration, *Handling of the generation of primary events in Gauss, the LHCb simulation framework*, *J. Phys. Conf. Ser.* **331** (2011) 032047 [INSPIRE].

[28] D.J. Lange, *The EvtGen particle decay simulation package*, *Nucl. Instrum. Meth. A* **462** (2001) 152 [INSPIRE].

[29] N. Davidson, T. Przedzinski and Z. Was, *PHOTOS interface in C++: technical and physics documentation*, *Comput. Phys. Commun.* **199** (2016) 86 [arXiv:1011.0937] [INSPIRE].

[30] J. Allison et al., *GEANT4 developments and applications*, *IEEE Trans. Nucl. Sci.* **53** (2006) 270 [INSPIRE].

[31] GEANT4 collaboration, *GEANT4 — a simulation toolkit*, *Nucl. Instrum. Meth. A* **506** (2003) 250 [INSPIRE].

[32] LHCb collaboration, *The LHCb simulation application, Gauss: design, evolution and experience*, *J. Phys. Conf. Ser.* **331** (2011) 032023 [INSPIRE].

[33] G.A. Cowan, D.C. Craik and M.D. Needham, *RapidSim: an application for the fast simulation of heavy-quark hadron decays*, *Comput. Phys. Commun.* **214** (2017) 239 [arXiv:1612.07489] [INSPIRE].

[34] Particle Data Group collaboration, *Review of particle physics*, *Phys. Rev. D* **110** (2024) 030001 [INSPIRE].

[35] P. Astier et al., *Kalman filter track fits and track break point analysis*, *Nucl. Instrum. Meth. A* **450** (2000) 138 [physics/9912034] [INSPIRE].

[36] Belle collaboration, *Study of the muon decay-in-flight in the $\tau^- \to \mu^- \bar{\nu}_\mu \nu_\tau$ to measure the Michel parameter ξ'*, *Phys. Rev. D* **108** (2023) 012003 [arXiv:2303.10574] [INSPIRE].

[37] CMS collaboration, *Identification of low-momentum muons in the CMS detector using multivariate techniques in proton-proton collisions at $\sqrt{s} = 13.6$ TeV*, 2025 *JINST* **20** P04021 [arXiv:2412.17590] [INSPIRE].

[38] L. Breiman, J. Friedman, R.A. Olshen and C.J. Stone, *Classification and regression trees*, Chapman and Hall/CRC, U.S.A. (2017) [DOI:10.1201/9781315139470] [INSPIRE].

[39] Y. Freund and R.E. Schapire, *A decision-theoretic generalization of on-line learning and an application to boosting*, *J. Comput. Syst. Sci.* **55** (1997) 119 [INSPIRE].

[40] H. Voss, A. Hocker, J. Stelzer and F. Tegenfeldt, *TMVA, the toolkit for multivariate data analysis with ROOT*, *PoS* **ACAT** (2007) 040 [INSPIRE].

[41] TMVA collaboration, *TMVA — toolkit for multivariate data analysis*, physics/0703039 [INSPIRE].

[42] H. Dembinski, M. Kenzie, C. Langenbruch and M. Schmelling, *Custom Orthogonal Weight functions (COWs) for event classification*, *Nucl. Instrum. Meth. A* **1040** (2022) 167270 [arXiv:2112.04574] [INSPIRE].

[43] M. De Cian, S. Farry, P. Seyfert and S. Stahl, *Fast neural-net based fake track rejection in the LHCb reconstruction*, LHCb-PUB-2017-011, CERN, Geneva, Switzerland (2017) [INSPIRE].

[44] W.D. Hulsbergen, *Decay chain fitting with a Kalman filter*, *Nucl. Instrum. Meth. A* **552** (2005) 566 [physics/0503191] [INSPIRE].

[45] M. Pivk and F.R. Le Diberder, *SPlot: a statistical tool to unfold data distributions*, *Nucl. Instrum. Meth. A* **555** (2005) 356 [physics/0402083] [INSPIRE].

[46] T. Chen and C. Guestrin, *XGBoost: a scalable tree boosting system*, in *Proceedings of the 22nd ACM SIGKDD international conference on knowledge discovery and data mining*, KDD '16, ACM, U.S.A. (2016), p. 785 [DOI:10.1145/2939672.2939785] [arXiv:1603.02754] [INSPIRE].

[47] LHCb collaboration, *Measurement of the $B^\pm$ production asymmetry and the CP asymmetry in $B^\pm \to J/\psi K^\pm$ decays*, *Phys. Rev. D* **95** (2017) 052005 [arXiv:1701.05501] [INSPIRE].

[48] G. Punzi, *Sensitivity optimization of multichannel searches for new signals*, arXiv:2011.11770 [INSPIRE].

[49] G. Punzi, *Sensitivity of searches for new signals and its optimization*, *eConf C* **030908** (2003) MODT002 [physics/0308063] [INSPIRE].

[50] C. Bishop, *Pattern recognition and machine learning (information science and statistics)*, (2007).

[51] T. Skwarnicki, *A study of the radiative CASCADE transitions between the Upsilon-Prime and Upsilon resonances*, Ph.D. thesis, INP, Cracow, Poland (1986) [INSPIRE].

[52] K.S. Cranmer, *Kernel estimation in high-energy physics*, *Comput. Phys. Commun.* **136** (2001) 198 [hep-ex/0011057] [INSPIRE].

[53] ATLAS collaboration, *Recommendations for the modeling of smooth backgrounds*, ATL-PHYS-PUB-2020-028, CERN, Geneva, Switzerland (2020) [INSPIRE].

[54] A.L. Read, *Presentation of search results: the CL_s technique*, *J. Phys. G* **28** (2002) 2693 [INSPIRE].

The LHCb collaboration

R. Aaij[38], A.S.W. Abdelmotteleb[57], C. Abellan Beteta[51], F. Abudinén[57], T. Ackernley[61], A. A. Adefisoye[69], B. Adeva[47], M. Adinolfi[55], P. Adlarson[84], C. Agapopoulou[14], C.A. Aidala[86], Z. Ajaltouni[11], S. Akar[11], K. Akiba[38], P. Albicocco[28], J. Albrecht[19,g], R. Aleksiejunas[79], F. Alessio[49], Z. Aliouche[63], P. Alvarez Cartelle[56], R. Amalric[16], S. Amato[3], J.L. Amey[55], Y. Amhis[14], L. An[6], L. Anderlini[27], M. Andersson[51], P. Andreola[51], M. Andreotti[26], S. Andres Estrada[83], A. Anelli[31,p,49], D. Ao[7], F. Archilli[37,w], Z. Areg[69], M. Argenton[26], S. Arguedas Cuendis[9,49], A. Artamonov[44], M. Artuso[69], E. Aslanides[13], R. Ataíde Da Silva[50], M. Atzeni[65], B. Audurier[12], J. A. Authier[15], D. Bacher[64], I. Bachiller Perea[50], S. Bachmann[22], M. Bachmayer[50], J.J. Back[57], P. Baladron Rodriguez[47], V. Balagura[15], A. Balboni[26], W. Baldini[26], L. Balzani[19], H. Bao[7], J. Baptista de Souza Leite[61], C. Barbero Pretel[47,12], M. Barbetti[27], I. R. Barbosa[70], R.J. Barlow[63], M. Barnyakov[25], S. Barsuk[14], W. Barter[59], J. Bartz[69], S. Bashir[40], B. Batsukh[5], P. B. Battista[14], A. Bay[50], A. Beck[65], M. Becker[19], F. Bedeschi[35], I.B. Bediaga[2], N. A. Behling[19], S. Belin[47], K. Belous[44], I. Belov[29], I. Belyaev[36], G. Benane[13], G. Bencivenni[28], E. Ben-Haim[16], A. Berezhnoy[44], R. Bernet[51], S. Bernet Andres[46], A. Bertolin[33], C. Betancourt[51], F. Betti[59], J. Bex[56], Ia. Bezshyiko[51], O. Bezshyyko[85], J. Bhom[41], M.S. Bieker[18], N.V. Biesuz[26], P. Billoir[16], A. Biolchini[38], M. Birch[62], F.C.R. Bishop[10], A. Bitadze[63], A. Bizzeti[27,q], T. Blake[57,c], F. Blanc[50], J.E. Blank[19], S. Blusk[69], V. Bocharnikov[44], J.A. Boelhauve[19], O. Boente Garcia[15], T. Boettcher[68], A. Bohare[59], A. Boldyrev[44], C.S. Bolognani[81], R. Bolzonella[26,m], R. B. Bonacci[1], N. Bondar[44,49], A. Bordelius[49], F. Borgato[33,49], S. Borghi[63], M. Borsato[31,p], J.T. Borsuk[82], E. Bottalico[61], S.A. Bouchiba[50], M. Bovill[64], T.J.V. Bowcock[61], A. Boyer[49], C. Bozzi[26], J. D. Brandenburg[87], A. Brea Rodriguez[50], N. Breer[19], J. Brodzicka[41], A. Brossa Gonzalo[47,†], J. Brown[61], D. Brundu[32], E. Buchanan[59], L. Buonincontri[33,r], M. Burgos Marcos[81], A.T. Burke[63], C. Burr[49], J.S. Butter[56], J. Buytaert[49], W. Byczynski[49], S. Cadeddu[32], H. Cai[74], Y. Cai[5], A. Caillet[16], R. Calabrese[26,m], S. Calderon Ramirez[9], L. Calefice[45], S. Cali[28], M. Calvi[31,p], M. Calvo Gomez[46], P. Camargo Magalhaes[2,a], J. I. Cambon Bouzas[47], P. Campana[28], D.H. Campora Perez[81], A.F. Campoverde Quezada[7], S. Capelli[31], L. Capriotti[26], R. Caravaca-Mora[9], A. Carbone[25,k], L. Carcedo Salgado[47], R. Cardinale[29,n], A. Cardini[32], P. Carniti[31], L. Carus[22], A. Casais Vidal[65], R. Caspary[22], G. Casse[61], M. Cattaneo[49], G. Cavallero[26], V. Cavallini[26,m], S. Celani[22], S. Cesare[30,o], A.J. Chadwick[61], I. Chahrour[86], H. Chang[4,d], M. Charles[16], Ph. Charpentier[49], E. Chatzianagnostou[38], R. Cheaib[78], M. Chefdeville[10], C. Chen[56], J. Chen[50], S. Chen[5], Z. Chen[7], M. Cherif[12], A. Chernov[41], S. Chernyshenko[53], X. Chiotopoulos[81], V. Chobanova[83], M. Chrzaszcz[41], A. Chubykin[44], V. Chulikov[28,36], P. Ciambrone[28], X. Cid Vidal[47], G. Ciezarek[49], P. Cifra[38], P.E.L. Clarke[59], M. Clemencic[49], H.V. Cliff[56], J. Closier[49], C. Cocha Toapaxi[22], V. Coco[49], J. Cogan[13], E. Cogneras[11], L. Cojocariu[43], S. Collaviti[50], P. Collins[49], T. Colombo[49], M. Colonna[19], A. Comerma-Montells[45], L. Congedo[24], J. Connaughton[57], A. Contu[32], N. Cooke[60], C. Coronel[66], I. Corredoira [12], A. Correia[16], G. Corti[49], J. Cottee Meldrum[55], B. Couturier[49], D.C. Craik[51], M. Cruz Torres[2,h], E. Curras Rivera[50], R. Currie[59],

JHEP12(2025)026

C.L. Da Silva[68], S. Dadabaev[44], L. Dai[71], X. Dai[4], E. Dall'Occo[49], J. Dalseno[83], C. D'Ambrosio[62], J. Daniel[11], P. d'Argent[24], G. Darze[3], A. Davidson[57], J.E. Davies[63], O. De Aguiar Francisco[63], C. De Angelis[32,l], F. De Benedetti[49], J. de Boer[38], K. De Bruyn[80], S. De Capua[63], M. De Cian[63], U. De Freitas Carneiro Da Graca[2,b], E. De Lucia[28], J.M. De Miranda[2], L. De Paula[3], M. De Serio[24,i], P. De Simone[28], F. De Vellis[19], J.A. de Vries[81], F. Debernardis[24], D. Decamp[10], S. Dekkers[1], L. Del Buono[16], B. Delaney[65], H.-P. Dembinski[19], J. Deng[8], V. Denysenko[51], O. Deschamps[11], F. Dettori[32,l], B. Dey[78], P. Di Nezza[28], I. Diachkov[44], S. Didenko[44], S. Ding[69], Y. Ding[50], L. Dittmann[22], V. Dobishuk[53], A. D. Docheva[60], A. Doheny[57], C. Dong[4,d], A.M. Donohoe[23], F. Dordei[32], A.C. dos Reis[2], A. D. Dowling[69], L. Dreyfus[13], W. Duan[72], P. Duda[82], M.W. Dudek[41], L. Dufour[49], V. Duk[34], P. Durante[49], M. M. Duras[82], J.M. Durham[68], O. D. Durmus[78], A. Dziurda[41], A. Dzyuba[44], S. Easo[58], E. Eckstein[18], U. Egede[1], A. Egorychev[44], V. Egorychev[44], S. Eisenhardt[59], E. Ejopu[63], L. Eklund[84], M. Elashri[66], J. Ellbracht[19], S. Ely[62], A. Ene[43], J. Eschle[69], S. Esen[22], T. Evans[38], F. Fabiano[32], S. Faghih[66], L.N. Falcao[2], B. Fang[7], R. Fantechi[35], L. Fantini[34,s], M. Faria[50], K. Farmer[59], D. Fazzini[31,p], L. Felkowski[82], M. Feng[5,7], M. Feo[19], A. Fernandez Casani[48], M. Fernandez Gomez[47], A.D. Fernez[67], F. Ferrari[25,k], F. Ferreira Rodrigues[3], M. Ferrillo[51], M. Ferro-Luzzi[49], S. Filippov[44], R.A. Fini[24], M. Fiorini[26,m], M. Firlej[40], K.L. Fischer[64], D.S. Fitzgerald[86], C. Fitzpatrick[63], T. Fiutowski[40], F. Fleuret[15], A. Fomin[52], M. Fontana[25], L. A. Foreman[63], R. Forty[49], D. Foulds-Holt[59], V. Franco Lima[3], M. Franco Sevilla[67], M. Frank[49], E. Franzoso[26,m], G. Frau[63], C. Frei[49], D.A. Friday[63], J. Fu[7], Q. Führing[19,g,56], T. Fulghesu[13], G. Galati[24], M.D. Galati[38], A. Gallas Torreira[47], D. Galli[25,k], S. Gambetta[59], M. Gandelman[3], P. Gandini[30], B. Ganie[63], H. Gao[7], R. Gao[64], T.Q. Gao[56], Y. Gao[8], Y. Gao[6], Y. Gao[8], L.M. Garcia Martin[50], P. Garcia Moreno[45], J. García Pardiñas[65], P. Gardner[67], K. G. Garg[8], L. Garrido[45], C. Gaspar[49], A. Gavrikov[33], L.L. Gerken[19], E. Gersabeck[20], M. Gersabeck[20], T. Gershon[57], S. Ghizzo[29,n], Z. Ghorbanimoghaddam[55], L. Giambastiani[33,r], F. I. Giasemis[16,f], V. Gibson[56], H.K. Giemza[42], A.L. Gilman[64], M. Giovannetti[28], A. Gioventù[45], L. Girardey[63,58], M.A. Giza[41], F.C. Glaser[14,22], V.V. Gligorov[16], C. Göbel[70], L. Golinka-Bezshyyko[85], E. Golobardes[46], D. Golubkov[44], A. Golutvin[62,49], S. Gomez Fernandez[45], W. Gomulka[40], I. Gonçales Vaz[49], F. Goncalves Abrantes[64], M. Goncerz[41], G. Gong[4,d], J. A. Gooding[19], I.V. Gorelov[44], C. Gotti[31], E. Govorkova[65], J.P. Grabowski[18], L.A. Granado Cardoso[49], E. Graugés[45], E. Graverini[50,u], L. Grazette[57], G. Graziani[27], A. T. Grecu[43], L.M. Greeven[38], N.A. Grieser[66], L. Grillo[60], S. Gromov[44], C. Gu[15], M. Guarise[26], L. Guerry[11], V. Guliaeva[44], P. A. Günther[22], A.-K. Guseinov[50], E. Gushchin[44], Y. Guz[6,49], T. Gys[49], K. Habermann[18], T. Hadavizadeh[1], C. Hadjivasiliou[67], G. Haefeli[50], C. Haen[49], S. Haken[56], G. Hallett[57], P.M. Hamilton[67], J. Hammerich[61], Q. Han[33], X. Han[22,49], S. Hansmann-Menzemer[22], L. Hao[7], N. Harnew[64], T. H. Harris[1], M. Hartmann[14], S. Hashmi[40], J. He[7,e], A. Hedes[63], F. Hemmer[49], C. Henderson[66], R. Henderson[14], R.D.L. Henderson[1], A.M. Hennequin[49], K. Hennessy[61], L. Henry[50], J. Herd[62], P. Herrero Gascon[22], J. Heuel[17], A. Hicheur[3], G. Hijano Mendizabal[51], J. Horswill[63], R. Hou[8], Y. Hou[11],

D. C. Houston[60], N. Howarth[61], J. Hu[72], W. Hu[7], X. Hu[4,d], W. Hulsbergen[38], R.J. Hunter[57], M. Hushchyn[44], D. Hutchcroft[61], M. Idzik[40], D. Ilin[44], P. Ilten[66], A. Iniukhin[44], A. Ishteev[44], K. Ivshin[44], H. Jage[17], S.J. Jaimes Elles[76,48,49], S. Jakobsen[49], E. Jans[38], B.K. Jashal[48], A. Jawahery[67], C. Jayaweera[54], V. Jevtic[19], Z. Jia[16], E. Jiang[67], X. Jiang[5,7], Y. Jiang[7], Y. J. Jiang[6], E. Jimenez Moya[9], N. Jindal[87], M. John[64], A. John Rubesh Rajan[23], D. Johnson[54], C.R. Jones[56], S. Joshi[42], B. Jost[49], J. Juan Castella[56], N. Jurik[49], I. Juszczak[41], D. Kaminaris[50], S. Kandybei[52], M. Kane[59], Y. Kang[4,d], C. Kar[11], M. Karacson[49], A. Kauniskangas[50], J.W. Kautz[66], M.K. Kazanecki[41], F. Keizer[49], M. Kenzie[56], T. Ketel[38], B. Khanji[69], A. Kharisova[44], S. Kholodenko[35,49], G. Khreich[14], T. Kirn[17], V.S. Kirsebom[31,p], O. Kitouni[65], S. Klaver[39], N. Kleijne[35,t], K. Klimaszewski[42], M.R. Kmiec[42], S. Koliiev[53], L. Kolk[19], A. Konoplyannikov[6], P. Kopciewicz[49], P. Koppenburg[38], A. Korchin[52], M. Korolev[44], I. Kostiuk[38], O. Kot[53], S. Kotriakhova, E. Kowalczyk[67], A. Kozachuk[44], P. Kravchenko[44], L. Kravchuk[44], O. Kravcov[79], M. Kreps[57], P. Krokovny[44], W. Krupa[69], W. Krzemien[42], O. Kshyvanskyi[53], S. Kubis[82], M. Kucharczyk[41], V. Kudryavtsev[44], E. Kulikova[44], A. Kupsc[84], V. Kushnir[52], B. Kutsenko[13], I. Kyryllin[52], D. Lacarrere[49], P. Laguarta Gonzalez[45], A. Lai[32], A. Lampis[32], D. Lancierini[62], C. Landesa Gomez[47], J.J. Lane[1], G. Lanfranchi[28], C. Langenbruch[22], J. Langer[19], O. Lantwin[44], T. Latham[57], F. Lazzari[35,u,49], C. Lazzeroni[54], R. Le Gac[13], H. Lee[61], R. Lefèvre[11], A. Leflat[44], S. Legotin[44], M. Lehuraux[57], E. Lemos Cid[49], O. Leroy[13], T. Lesiak[41], E. D. Lesser[49], B. Leverington[22], A. Li[4,d], C. Li[4], C. Li[13], H. Li[72], J. Li[8], K. Li[75], L. Li[63], M. Li[8], P. Li[7], P.-R. Li[73], Q. Li[5,7], T. Li[71], T. Li[72], Y. Li[8], Y. Li[5], Y. Li[4], Z. Lian[4,d], Q. Liang[8], X. Liang[69], S. Libralon[48], A. L. Lightbody[12], C. Lin[7], T. Lin[58], R. Lindner[49], H. Linton[62], R. Litvinov[32], D. Liu[8], F. L. Liu[1], G. Liu[72], K. Liu[73], S. Liu[5,7], W. Liu[8], Y. Liu[59], Y. Liu[73], Y. L. Liu[62], G. Loachamin Ordonez[70], A. Lobo Salvia[45], A. Loi[32], T. Long[56], F. C. L. Lopes[2,a], J.H. Lopes[3], A. Lopez Huertas[45], C. Lopez Iribarnegaray[47], S. López Soliño[47], Q. Lu[15], C. Lucarelli[49], D. Lucchesi[33,r], M. Lucio Martinez[48], Y. Luo[6], A. Lupato[33,j], E. Luppi[26,m], K. Lynch[23], X.-R. Lyu[7], G. M. Ma[4,d], S. Maccolini[19], F. Machefert[14], F. Maciuc[43], B. Mack[69], I. Mackay[64], L. M. Mackey[69], L.R. Madhan Mohan[56], M. J. Madurai[54], D. Magdalinski[38], D. Maisuzenko[44], J.J. Malczewski[41], S. Malde[64], L. Malentacca[49], A. Malinin[44], T. Maltsev[44], G. Manca[32,l], G. Mancinelli[13], C. Mancuso[14], R. Manera Escalero[45], F. M. Manganella[37], D. Manuzzi[25], D. Marangotto[30,o], J.F. Marchand[10], R. Marchevski[50], U. Marconi[25], E. Mariani[16], S. Mariani[49], C. Marin Benito[45], J. Marks[22], A.M. Marshall[55], L. Martel[64], G. Martelli[34], G. Martellotti[36], L. Martinazzoli[49], M. Martinelli[31,p], D. Martinez Gomez[80], D. Martinez Santos[83], F. Martinez Vidal[48], A. Martorell i Granollers[46], A. Massafferri[2], R. Matev[49], A. Mathad[49], V. Matiunin[44], C. Matteuzzi[69], K.R. Mattioli[15], A. Mauri[62], E. Maurice[15], J. Mauricio[45], P. Mayencourt[50], J. Mazorra de Cos[48], M. Mazurek[42], M. McCann[62], T.H. McGrath[63], N.T. McHugh[60], A. McNab[63], R. McNulty[23], B. Meadows[66], G. Meier[19], D. Melnychuk[42], D. Mendoza Granada[16], F. M. Meng[4,d], M. Merk[38,81], A. Merli[50,30], L. Meyer Garcia[67], D. Miao[5,7], H. Miao[7], M. Mikhasenko[77], D.A. Milanes[76,z], A. Minotti[31,p], E. Minucci[28],

T. Miralles[11], B. Mitreska[19], D.S. Mitzel[19], A. Modak[58], L. Moeser[19], R.D. Moise[17], E. F. Molina Cardenas[86], T. Mombächer[49], M. Monk[57,1], S. Monteil[11], A. Morcillo Gomez[47], G. Morello[28], M.J. Morello[35,t], M.P. Morgenthaler[22], J. Moron[40], W. Morren[38], A.B. Morris[49], A.G. Morris[13], R. Mountain[69], H. Mu[4,d], Z. M. Mu[6], E. Muhammad[57], F. Muheim[59], M. Mulder[80], K. Müller[51], F. Muñoz-Rojas[9], R. Murta[62], V. Mytrochenko[52], P. Naik[61], T. Nakada[50], R. Nandakumar[58], T. Nanut[49], I. Nasteva[3], M. Needham[59], E. Nekrasova[44], N. Neri[30,o], S. Neubert[18], N. Neufeld[49], P. Neustroev[44], J. Nicolini[49], D. Nicotra[81], E.M. Niel[15], N. Nikitin[44], Q. Niu[73], P. Nogarolli[3], P. Nogga[18], C. Normand[55], J. Novoa Fernandez[47], G. Nowak[66], C. Nunez[86], H. N. Nur[60], A. Oblakowska-Mucha[40], V. Obraztsov[44], T. Oeser[17], A. Okhotnikov[44], O. Okhrimenko[53], R. Oldeman[32,l], F. Oliva[59,49], E. Olivart Pino[45], M. Olocco[19], C.J.G. Onderwater[81], R.H. O'Neil[49], J.S. Ordonez Soto[11], D. Osthues[19], J.M. Otalora Goicochea[3], P. Owen[51], A. Oyanguren[48], O. Ozcelik[49], F. Paciolla[35,x], A. Padee[42], K.O. Padeken[18], B. Pagare[47], T. Pajero[49], A. Palano[24], M. Palutan[28], C. Pan[74], X. Pan[4,d], S. Panebianco[12], G. Panshin[5], L. Paolucci[57], A. Papanestis[58], M. Pappagallo[24,i], L.L. Pappalardo[26], C. Pappenheimer[66], C. Parkes[63], D. Parmar[77], B. Passalacqua[26,m], G. Passaleva[27], D. Passaro[35,t,49], A. Pastore[24], M. Patel[62], J. Patoc[64], C. Patrignani[25,k], A. Paul[69], C.J. Pawley[81], A. Pellegrino[38], J. Peng[5,7], X. Peng[73], M. Pepe Altarelli[28], S. Perazzini[25], D. Pereima[44], H. Pereira Da Costa[68], M. Pereira Martinez[47], A. Pereiro Castro[47], C. Perez[46], P. Perret[11], A. Perrevoort[80], A. Perro[49,13], M.J. Peters[66], K. Petridis[55], A. Petrolini[29,n], J. P. Pfaller[66], H. Pham[69], L. Pica[35,t], M. Piccini[34], L. Piccolo[32], B. Pietrzyk[10], G. Pietrzyk[14], R. N. Pilato[61], D. Pinci[36], F. Pisani[49], M. Pizzichemi[31,p,49], V. M. Placinta[43], M. Plo Casasus[47], T. Poeschl[49], F. Polci[16], M. Poli Lener[28], A. Poluektov[13], N. Polukhina[44], I. Polyakov[63], E. Polycarpo[3], S. Ponce[49], D. Popov[7,49], S. Poslavskii[44], K. Prasanth[59], C. Prouve[83], D. Provenzano[32,l,49], V. Pugatch[53], G. Punzi[35,u], S. Qasim[51], Q. Q. Qian[6], W. Qian[7], N. Qin[4,d], S. Qu[4,d], R. Quagliani[49], R.I. Rabadan Trejo[57], R. Racz[79], J.H. Rademacker[55], M. Rama[35], M. Ramírez García[86], V. Ramos De Oliveira[70], M. Ramos Pernas[57], M.S. Rangel[3], F. Ratnikov[44], G. Raven[39], M. Rebollo De Miguel[48], F. Redi[30,j], J. Reich[55], F. Reiss[20], Z. Ren[7], P.K. Resmi[64], M. Ribalda Galvez[45], R. Ribatti[50], G. Ricart[15,12], D. Riccardi[35,t], S. Ricciardi[58], K. Richardson[65], M. Richardson-Slipper[56], K. Rinnert[61], P. Robbe[14,49], G. Robertson[60], E. Rodrigues[61], A. Rodriguez Alvarez[45], E. Rodriguez Fernandez[47], J.A. Rodriguez Lopez[76], E. Rodriguez Rodriguez[49], J. Roensch[19], A. Rogachev[44], A. Rogovskiy[58], D.L. Rolf[19], P. Roloff[49], V. Romanovskiy[66], A. Romero Vidal[47], G. Romolini[26,49], F. Ronchetti[50], T. Rong[6], M. Rotondo[28], S. R. Roy[22], M.S. Rudolph[69], M. Ruiz Diaz[22], R.A. Ruiz Fernandez[47], J. Ruiz Vidal[81], J. J. Saavedra-Arias[9], J.J. Saborido Silva[47], S. E. R. Sacha Emile R.[49], R. Sadek[15], N. Sagidova[44], D. Sahoo[78], N. Sahoo[54], B. Saitta[32,l], M. Salomoni[31,49,p], I. Sanderswood[48], R. Santacesaria[36], C. Santamarina Rios[47], M. Santimaria[28], L. Santoro[2], E. Santovetti[37], A. Saputi[26,49], D. Saranin[44], A. Sarnatskiy[80], G. Sarpis[49], M. Sarpis[79], C. Satriano[36,v], A. Satta[37], M. Saur[73], D. Savrina[44], H. Sazak[17], F. Sborzacchi[49,28], A. Scarabotto[19], S. Schael[17], S. Scherl[61], M. Schiller[22], H. Schindler[49], M. Schmelling[21], B. Schmidt[49], S. Schmitt[17],

JHEP12(2025)026

H. Schmitz[18], O. Schneider[50], A. Schopper[62], N. Schulte[19], M.H. Schune[14], G. Schwering[17], B. Sciascia[28], A. Sciuccati[49], I. Segal[77], S. Sellam[47], A. Semennikov[44], T. Senger[51], M. Senghi Soares[39], A. Sergi[29,n], N. Serra[51], L. Sestini[27], A. Seuthe[19], B. Sevilla Sanjuan[46], Y. Shang[6], D.M. Shangase[86], M. Shapkin[44], R. S. Sharma[69], I. Shchemerov[44], L. Shchutska[50], T. Shears[61], L. Shekhtman[44], Z. Shen[38], S. Sheng[5,7], V. Shevchenko[44], B. Shi[7], Q. Shi[7], W. S. Shi[72], Y. Shimizu[14], E. Shmanin[25], R. Shorkin[44], J.D. Shupperd[69], R. Silva Coutinho[69], G. Simi[33,r], S. Simone[24,i], M. Singha[78], N. Skidmore[57], T. Skwarnicki[69], M.W. Slater[54], E. Smith[65], K. Smith[68], M. Smith[62], L. Soares Lavra[59], M.D. Sokoloff[66], F.J.P. Soler[60], A. Solomin[55], A. Solovev[44], N. S. Sommerfeld[18], R. Song[1], Y. Song[50], Y. Song[4,d], Y. S. Song[6], F.L. Souza De Almeida[69], B. Souza De Paula[3], K.M. Sowa[40], E. Spadaro Norella[29,n], E. Spedicato[25], J.G. Speer[19], P. Spradlin[60], V. Sriskaran[49], F. Stagni[49], M. Stahl[77], S. Stahl[49], S. Stanislaus[64], M. Stefaniak[87], E.N. Stein[49], O. Steinkamp[51], H. Stevens[19], D. Strekalina[44], Y. Su[7], F. Suljik[64], J. Sun[32], J. Sun[63], L. Sun[74], D. Sundfeld[2], W. Sutcliffe[51], K. Swientek[40], F. Swystun[56], A. Szabelski[42], T. Szumlak[40], Y. Tan[4,d], Y. Tang[74], Y. T. Tang[7], M.D. Tat[22], J. A. Teijeiro Jimenez[47], A. Terentev[44], F. Terzuoli[35,x], F. Teubert[49], E. Thomas[49], D.J.D. Thompson[54], A. R. Thomson-Strong[59], H. Tilquin[62], V. Tisserand[11], S. T'Jampens[10], M. Tobin[5,49], T. T. Todorov[20], L. Tomassetti[26,m], G. Tonani[30], X. Tong[6], T. Tork[30], D. Torres Machado[2], L. Toscano[19], D.Y. Tou[4,d], C. Trippl[46], G. Tuci[22], N. Tuning[38], L.H. Uecker[22], A. Ukleja[40], D.J. Unverzagt[22], A. Upadhyay[49], B. Urbach[59], A. Usachov[39], A. Ustyuzhanin[44], U. Uwer[22], V. Vagnoni[25,49], V. Valcarce Cadenas[47], G. Valenti[25], N. Valls Canudas[49], J. van Eldik[49], H. Van Hecke[68], E. van Herwijnen[62], C.B. Van Hulse[47,aa], R. Van Laak[50], M. van Veghel[38], G. Vasquez[51], R. Vazquez Gomez[45], P. Vazquez Regueiro[47], C. Vázquez Sierra[83], S. Vecchi[26], J.J. Velthuis[55], M. Veltri[27,y], A. Venkateswaran[50], M. Verdoglia[32], M. Vesterinen[57], W. Vetens[69], D. Vico Benet[64], P. Vidrier Villalba[45], M. Vieites Diaz[47], X. Vilasis-Cardona[46], E. Vilella Figueras[61], A. Villa[25], P. Vincent[16], B. Vivacqua[3], F.C. Volle[54], D. vom Bruch[13], N. Voropaev[44], K. Vos[81], C. Vrahas[59], J. Wagner[19], J. Walsh[35], E.J. Walton[1,57], G. Wan[6], A. Wang[7], B. Wang[5], C. Wang[22], G. Wang[8], H. Wang[73], J. Wang[6], J. Wang[5], J. Wang[4,d], J. Wang[74], M. Wang[49], N. W. Wang[7], R. Wang[55], X. Wang[8], X. Wang[72], X. W. Wang[62], Y. Wang[75], Y. Wang[6], Y. H. Wang[73], Z. Wang[14], Z. Wang[4,d], Z. Wang[30], J.A. Ward[57], M. Waterlaat[49], N.K. Watson[54], D. Websdale[62], Y. Wei[6], J. Wendel[83], B.D.C. Westhenry[55], C. White[56], M. Whitehead[60], E. Whiter[54], A.R. Wiederhold[63], D. Wiedner[19], M. A. Wiegertjes[38], C. Wild[64], G. Wilkinson[64,49], M.K. Wilkinson[66], M. Williams[65], M. J. Williams[49], M.R.J. Williams[59], R. Williams[56], S. Williams[55], Z. Williams[55], F.F. Wilson[58], M. Winn[12], W. Wislicki[42], M. Witek[41], L. Witola[19], T. Wolf[22], E. Wood[56], G. Wormser[14], S.A. Wotton[56], H. Wu[69], J. Wu[8], X. Wu[74], Y. Wu[6,56], Z. Wu[7], K. Wyllie[49], S. Xian[72], Z. Xiang[5], Y. Xie[8], T. X. Xing[30], A. Xu[35,t], L. Xu[4,d], L. Xu[4,d], M. Xu[49], Z. Xu[49], Z. Xu[7], Z. Xu[5], K. Yang[62], X. Yang[6], Y. Yang[15], Z. Yang[6], V. Yeroshenko[14], H. Yeung[63], H. Yin[8], X. Yin[7], C. Y. Yu[6], J. Yu[71], X. Yuan[5], Y Yuan[5,7], E. Zaffaroni[50], M. Zavertyaev[21], M. Zdybal[41], F. Zenesini[25], C. Zeng[5,7], M. Zeng[4,d], C. Zhang[6], D. Zhang[8], J. Zhang[7], L. Zhang[4,d],

JHEP12(2025)026

R. Zhang [8], S. Zhang [71], S. Zhang [64], Y. Zhang [6], Y. Z. Zhang [4,d], Z. Zhang [4,d], Y. Zhao [22], A. Zhelezov [22], S. Z. Zheng [6], X. Z. Zheng [4,d], Y. Zheng [7], T. Zhou [6], X. Zhou [8], Y. Zhou [7], V. Zhovkovska [57], L. Z. Zhu [7], X. Zhu [4,d], X. Zhu [8], Y. Zhu [17], V. Zhukov [17], J. Zhuo [48], Q. Zou [5,7], D. Zuliani [33,r], G. Zunica [50]

[1] *School of Physics and Astronomy, Monash University, Melbourne, Australia*
[2] *Centro Brasileiro de Pesquisas Físicas (CBPF), Rio de Janeiro, Brazil*
[3] *Universidade Federal do Rio de Janeiro (UFRJ), Rio de Janeiro, Brazil*
[4] *Department of Engineering Physics, Tsinghua University, Beijing, China*
[5] *Institute Of High Energy Physics (IHEP), Beijing, China*
[6] *School of Physics State Key Laboratory of Nuclear Physics and Technology, Peking University, Beijing, China*
[7] *University of Chinese Academy of Sciences, Beijing, China*
[8] *Institute of Particle Physics, Central China Normal University, Wuhan, Hubei, China*
[9] *Consejo Nacional de Rectores (CONARE), San Jose, Costa Rica*
[10] *Université Savoie Mont Blanc, CNRS, IN2P3-LAPP, Annecy, France*
[11] *Université Clermont Auvergne, CNRS/IN2P3, LPC, Clermont-Ferrand, France*
[12] *Université Paris-Saclay, Centre d'Etudes de Saclay (CEA), IRFU, Saclay, France, Gif-Sur-Yvette, France*
[13] *Aix Marseille Univ, CNRS/IN2P3, CPPM, Marseille, France*
[14] *Université Paris-Saclay, CNRS/IN2P3, IJCLab, Orsay, France*
[15] *Laboratoire Leprince-Ringuet, CNRS/IN2P3, Ecole Polytechnique, Institut Polytechnique de Paris, Palaiseau, France*
[16] *LPNHE, Sorbonne Université, Paris Diderot Sorbonne Paris Cité, CNRS/IN2P3, Paris, France*
[17] *I. Physikalisches Institut, RWTH Aachen University, Aachen, Germany*
[18] *Universität Bonn — Helmholtz-Institut für Strahlen und Kernphysik, Bonn, Germany*
[19] *Fakultät Physik, Technische Universität Dortmund, Dortmund, Germany*
[20] *Physikalisches Institut, Albert-Ludwigs-Universität Freiburg, Freiburg, Germany*
[21] *Max-Planck-Institut für Kernphysik (MPIK), Heidelberg, Germany*
[22] *Physikalisches Institut, Ruprecht-Karls-Universität Heidelberg, Heidelberg, Germany*
[23] *School of Physics, University College Dublin, Dublin, Ireland*
[24] *INFN Sezione di Bari, Bari, Italy*
[25] *INFN Sezione di Bologna, Bologna, Italy*
[26] *INFN Sezione di Ferrara, Ferrara, Italy*
[27] *INFN Sezione di Firenze, Firenze, Italy*
[28] *INFN Laboratori Nazionali di Frascati, Frascati, Italy*
[29] *INFN Sezione di Genova, Genova, Italy*
[30] *INFN Sezione di Milano, Milano, Italy*
[31] *INFN Sezione di Milano-Bicocca, Milano, Italy*
[32] *INFN Sezione di Cagliari, Monserrato, Italy*
[33] *INFN Sezione di Padova, Padova, Italy*
[34] *INFN Sezione di Perugia, Perugia, Italy*
[35] *INFN Sezione di Pisa, Pisa, Italy*
[36] *INFN Sezione di Roma La Sapienza, Roma, Italy*
[37] *INFN Sezione di Roma Tor Vergata, Roma, Italy*
[38] *Nikhef National Institute for Subatomic Physics, Amsterdam, Netherlands*
[39] *Nikhef National Institute for Subatomic Physics and VU University Amsterdam, Amsterdam, Netherlands*
[40] *AGH — University of Krakow, Faculty of Physics and Applied Computer Science, Kraków, Poland*
[41] *Henryk Niewodniczanski Institute of Nuclear Physics Polish Academy of Sciences, Kraków, Poland*
[42] *National Center for Nuclear Research (NCBJ), Warsaw, Poland*
[43] *Horia Hulubei National Institute of Physics and Nuclear Engineering, Bucharest-Magurele, Romania*
[44] *Authors affiliated with an institute formerly covered by a cooperation agreement with CERN.*
[45] *ICCUB, Universitat de Barcelona, Barcelona, Spain*
[46] *La Salle, Universitat Ramon Llull, Barcelona, Spain*

JHEP12(2025)026

[47] Instituto Galego de Física de Altas Enerxías (IGFAE), Universidade de Santiago de Compostela, Santiago de Compostela, Spain
[48] Instituto de Fisica Corpuscular, Centro Mixto Universidad de Valencia — CSIC, Valencia, Spain
[49] European Organization for Nuclear Research (CERN), Geneva, Switzerland
[50] Institute of Physics, Ecole Polytechnique Fédérale de Lausanne (EPFL), Lausanne, Switzerland
[51] Physik-Institut, Universität Zürich, Zürich, Switzerland
[52] NSC Kharkiv Institute of Physics and Technology (NSC KIPT), Kharkiv, Ukraine
[53] Institute for Nuclear Research of the National Academy of Sciences (KINR), Kyiv, Ukraine
[54] School of Physics and Astronomy, University of Birmingham, Birmingham, United Kingdom
[55] H.H. Wills Physics Laboratory, University of Bristol, Bristol, United Kingdom
[56] Cavendish Laboratory, University of Cambridge, Cambridge, United Kingdom
[57] Department of Physics, University of Warwick, Coventry, United Kingdom
[58] STFC Rutherford Appleton Laboratory, Didcot, United Kingdom
[59] School of Physics and Astronomy, University of Edinburgh, Edinburgh, United Kingdom
[60] School of Physics and Astronomy, University of Glasgow, Glasgow, United Kingdom
[61] Oliver Lodge Laboratory, University of Liverpool, Liverpool, United Kingdom
[62] Imperial College London, London, United Kingdom
[63] Department of Physics and Astronomy, University of Manchester, Manchester, United Kingdom
[64] Department of Physics, University of Oxford, Oxford, United Kingdom
[65] Massachusetts Institute of Technology, Cambridge, MA, United States
[66] University of Cincinnati, Cincinnati, OH, United States
[67] University of Maryland, College Park, MD, United States
[68] Los Alamos National Laboratory (LANL), Los Alamos, NM, United States
[69] Syracuse University, Syracuse, NY, United States
[70] Pontifícia Universidade Católica do Rio de Janeiro (PUC-Rio), Rio de Janeiro, Brazil, associated to [3]
[71] School of Physics and Electronics, Hunan University, Changsha City, China, associated to [8]
[72] Guangdong Provincial Key Laboratory of Nuclear Science, Guangdong-Hong Kong Joint Laboratory of Quantum Matter, Institute of Quantum Matter, South China Normal University, Guangzhou, China, associated to [4]
[73] Lanzhou University, Lanzhou, China, associated to [5]
[74] School of Physics and Technology, Wuhan University, Wuhan, China, associated to [4]
[75] Henan Normal University, Xinxiang, China, associated to [8]
[76] Departamento de Fisica, Universidad Nacional de Colombia, Bogota, Colombia, associated to [16]
[77] Ruhr Universitaet Bochum, Fakultaet f. Physik und Astronomie, Bochum, Germany, associated to [19]
[78] Eotvos Lorand University, Budapest, Hungary, associated to [49]
[79] Faculty of Physics, Vilnius University, Vilnius, Lithuania, associated to [20]
[80] Van Swinderen Institute, University of Groningen, Groningen, Netherlands, associated to [38]
[81] Universiteit Maastricht, Maastricht, Netherlands, associated to [38]
[82] Tadeusz Kosciuszko Cracow University of Technology, Cracow, Poland, associated to [41]
[83] Universidade da Coruña, A Coruña, Spain, associated to [46]
[84] Department of Physics and Astronomy, Uppsala University, Uppsala, Sweden, associated to [60]
[85] Taras Schevchenko University of Kyiv, Faculty of Physics, Kyiv, Ukraine, associated to [14]
[86] University of Michigan, Ann Arbor, MI, United States, associated to [69]
[87] Ohio State University, Columbus, United States, associated to [68]

[a] Universidade Estadual de Campinas (UNICAMP), Campinas, Brazil
[b] Centro Federal de Educacão Tecnológica Celso Suckow da Fonseca, Rio De Janeiro, Brazil
[c] Department of Physics and Astronomy, University of Victoria, Victoria, Canada
[d] Center for High Energy Physics, Tsinghua University, Beijing, China
[e] Hangzhou Institute for Advanced Study, UCAS, Hangzhou, China
[f] LIP6, Sorbonne Université, Paris, France
[g] Lamarr Institute for Machine Learning and Artificial Intelligence, Dortmund, Germany
[h] Universidad Nacional Autónoma de Honduras, Tegucigalpa, Honduras

JHEP12(2025)026

[i] Università di Bari, Bari, Italy
[j] Università di Bergamo, Bergamo, Italy
[k] Università di Bologna, Bologna, Italy
[l] Università di Cagliari, Cagliari, Italy
[m] Università di Ferrara, Ferrara, Italy
[n] Università di Genova, Genova, Italy
[o] Università degli Studi di Milano, Milano, Italy
[p] Università degli Studi di Milano-Bicocca, Milano, Italy
[q] Università di Modena e Reggio Emilia, Modena, Italy
[r] Università di Padova, Padova, Italy
[s] Università di Perugia, Perugia, Italy
[t] Scuola Normale Superiore, Pisa, Italy
[u] Università di Pisa, Pisa, Italy
[v] Università della Basilicata, Potenza, Italy
[w] Università di Roma Tor Vergata, Roma, Italy
[x] Università di Siena, Siena, Italy
[y] Università di Urbino, Urbino, Italy
[z] Universidad de Ingeniería y Tecnología (UTEC), Lima, Peru
[aa] Universidad de Alcalá, Alcalá de Henares, Spain
[†] Deceased